A fast, new method to enhance the enantiomeric purity of non-racemic mixtures: self-disproportionation of enantiomers in the gas antisolvent fractionation of chlorine-substituted mandelic acid derivatives

Márton Kőrösi[a]; János Madarász[b]; Tamás Sohajda[c]; Edit Székely[a*]

[a]*Budapest University of Technology and Economics; Budapest, Hungary; Department of Chemical and Environmental Process Engineering; 3. Műegyetem rakpart, H-1111, Budapest, Hungary*

[b]*Budapest University of Technology and Economics; Budapest, Hungary; Department of Inorganic and Analytical Chemistry; 3. Műegyetem rakpart, H-1111, Budapest, Hungary*

[c]*Cyclolab Cyclodextrin Research and Development Ltd.; 7. Illatos út; 1097 Budapest, Hungary*

** corresponding author: sz-edit@mail.bme.hu*

Abstract

Gas antisolvent precipitation is a particle formation technique, when typically pressurized carbon dioxide is added to an organic solution resulting in immediate and high oversaturation and precipitation of fine particles. Provided that a reasonable share of the originally dissolved material remains dissolved in the carbon dioxide – organic mixed solvent, these components can be extracted during the washing phase. Then the method is called gas antisolvent fractionation (GASF). GASF has been applied for the first time for enantiomeric enrichment of non-racemic mixtures, demonstrated on the example of chlorinated mandelic acid derivatives. Due to self-disproportionation of enantiomers, the precipitated solid and the extracted fractions have different enantiomeric excesses if GASF is done on a non-racemic mixture. However, there is a limit in the enantiomeric excess (*ee*) that can be achieved correlating strongly with the atmospheric melting eutectic behavior of the compounds. Thus, if initial enantiomeric mixtures have a higher than eutectic *ee*, a >99% *ee* can be reached in the crystalline product. The strong correlation between the high-pressure experiments and the atmospheric melting eutectic behavior suggests that despite the very large oversaturation during the antisolvent precipitation, the composition of the products (i.e. the crystalline and the extracted phases) is thermodynamically determined. Technological advantages such as short operational time, or the possibility of controlling the crystal morphology suggest that the development of an efficient technique of enantiomeric purification is possible based on gas antisolvent fractionation.

Keywords: supercritical carbon dioxide; eutectic; antisolvent precipitation; enantiomeric enrichment; chiral; optical purity; capillary electrophoresis; self-disproportionation of enantiomers

1. Introduction

The need for the production of enantiopure compounds in the pharmaceutical industry, manufacturing of agrochemicals and in the food industry is the driving force of the development of new methods of enantiomeric enrichment.

Enantiomeric enrichment of non-racemic mixtures can be carried out without the addition of any chiral selector. When the *ee* values of the separated products differ from each other and that

of the starting material, we talk about self-disproportionation of enantiomers (SDE).[1,2] The phenomenon has been observed in separation techniques like for example sublimation[3] or high-performance liquid chromatography (HPLC) with achiral moving and stationary phases[4]. Among the techniques aiming the enhancement of the enantiomeric purity of non-racemic mixtures, recrystallization is a very simple way to enhance the optical purity of the target compound. SDE can also be observed under these circumstances. In case of racemic compounds, the atmospheric recrystallization-based enantiomeric enrichment process is limited by the eutectic behavior of dissolution, which is close to the eutectic composition observable in the melting point phase diagrams. The crystalline phase formed in a solution of a lower than eutectic enantiomeric purity (i.e. $ee_0 < ee_{eu}$) has typically lower optical purity than the initial *ee*, while the mother liquor contains the enantiomerically enriched material. Starting from over the eutectic composition ($ee_0 > ee_{eu}$) the opposite happens. Conglomerate forming compounds do not exhibit such boundaries. The strong correlation of the limiting *ee* value in enantiomeric enrichment with the eutectic *ee* of the binary melting point phase diagram was described by Faigl et al. through several recrystallization processes. The authors explain their results as the consequence of thermodynamic control during the recrystallization experiments.[5]

Traditional recrystallization processes are often slow, and use large amounts of organic solvents. Gas antisolvent (GAS) precipitation and supercritical antisolvent precipitation (SAS) both using supercritical carbon dioxide as an antisolvent are widely studied and applied techniques to recrystallize various compounds. Antisolvent processes are not only fast and eco-friendly (reducing the amount of organic solvent needed), but also offer the possibility to produce fine powders with narrow particle size distribution in the micrometer main particle diameter range. The morphology (i.e. the crystal habit) can also be influenced by the operational parameters, however, this advantage can only be exploited in a scaled-up equipment. Besides the advantages, safety issues and higher investment costs regarding the high pressure unit operations have to be taken into consideration.[6–9] GAS fractionation is a combination of the GAS precipitation and separation of the impurities by the following supercritical fluid extraction, it is also referred to in the literature as supercritical antisolvent extraction[10–12], supercritical antisolvent fractionation[13] etc. GAS and SAS have already been used as separation methods in chiral resolutions carried out by diastereomeric salt formation.[14,15] The technique is now presented for the first time for enantiomeric enrichment based on SDE.

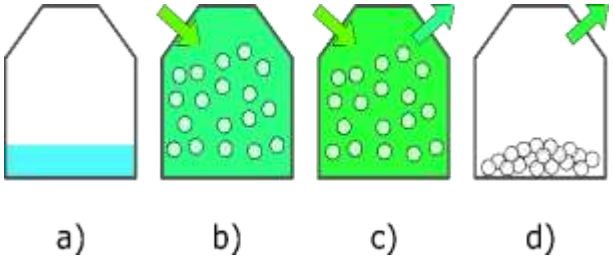

Figure 1. Stepwise depiction of the gas antisolvent fractionation process
a) The compounds to be precipitated (and separated) are filled into the autoclave as a solution.
b) Carbon dioxide is introduced, resulting in a polarity change and precipitation.
c) The dissolved components are extracted using pure supercritical carbon dioxide and can be collected in a solvent trap (not pictured).
d) The crystalline product can be recovered after depressurization.

During the GAS fractionation process (Fig. 1.), the aim is to achieve partial precipitation of a compound dissolved in an organic solvent. First, a nearly saturated solution of the starting material needs to be prepared, and filled into a suitable high pressure vessel (Fig. 1. a)). Then carbon dioxide is introduced that is dissolved by the organic solvent. Thus, because of the expansion and polarity drop of the solvent, its solvent power is sharply reduced, resulting in (partial) precipitation of polar components (Fig. 1. b)). By choosing appropriate operational parameters (i.e. pressure, temperature and organic solvent concentration) a homogenous fluid phase can be achieved over the precipitate. The dissolved portion of the starting material together with the organic solvent can be extracted using pure carbon dioxide (Fig. 1. c)). After depressurization of the equipment, the crystalline product can be recovered (Fig. 1. d)).

We aimed to develop a method to enhance the enantiomeric purity of non-racemic mixtures of chlorinated mandelic acid derivatives (Fig. 2.) based on their recrystallization by GASF. Mandelic acid derivatives are often used as resolving agents or intermediates in the pharmaceutical or agrochemical industries to introduce optically active chiral centers in the molecules.[16–20] We also investigated the possible correlation between the limits of enantiomeric enrichment observable in the products' *ee* – initial *ee* diagrams and the atmospheric melting

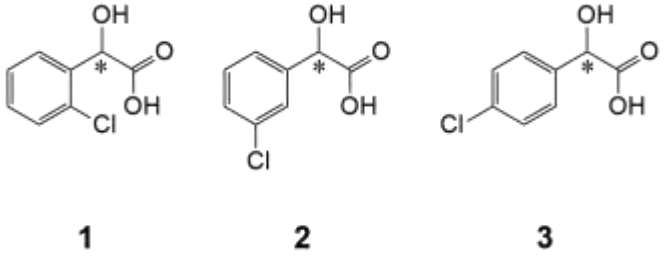

Figure 2. The studied mandelic acid derivatives
1 2-chloromandelic acid
2 3-chloromandelic acid
3 4-chloromandelic acid

point phase diagrams in order to gain further understanding in the mechanism of the chiral discrimination.

2. Results and discussion

Melting point phase equilibria diagrams of **1** and **2** have already been reported in the literature.[21,22] DSC measurements were carried out to confirm the data obtained from the references. The experimental phase equilibria diagram of 4-chloromandelic acid was however not available in the public literature, only the melting points and fusion enthalpies of the single enantiomers and of the racemate are published.[23,24] Experimental and literature data of atmospheric melting temperatures and fusion enthalpies are summarized in Table 1. Own experimental values were used for the modeling of the melting point phase equilibrium curves pictured in the upper sections of Figs. 3-5.

Compound	**1**	**2**	**3**
Measured data			
T_{rac} [K]	362	387	393
T_R [K]	393	378	393
ΔH_{rac} [J/mol]	21588	24609	25749
ΔH_R [J/mol]	24033	23251	21345
Data obtained from the literature			
T_{rac} [K]	363 [22]	390 [21]	393 [24]; 394 [23]
T_R [K]	392 [22]	379 [21]	393 [24]; 394 [23]
ΔH_{rac} [J/mol]	23137 [22]	27980 [21]	16200 [24]; 27200 [23]
ΔH_R [J/mol]	24947 [22]	26240 [21]	27100 [24]; 23000 [23]

Table 1. Melting temperature and fusion enthalpy data of racemic and enantiopure **1**, **2**, and **3**. Indices rac and R refer to racemic and enantiopure, respectively.

To model the phase equilibrium behavior of the acids, the Prigogin–Defay equation (1) was used at *ee* values lower than the eutectic *ee* and the Schröder–van-Laar equation (2) was used at *ee* values higher than the eutectic *ee* of the corresponding acid. [22]

$$\ln[4 \cdot X_R \cdot (1 - X_R)] = \frac{2 \cdot \Delta H_{rac}}{R} \cdot \left(\frac{1}{T_{rac}} - \frac{1}{T}\right) \qquad (1)$$

$$\ln X_R = \frac{\Delta H_R}{R} \cdot \left(\frac{1}{T_R} - \frac{1}{T}\right) \qquad (2)$$

Where X_R denotes the molar fraction of the (*R*) enantiomer. ΔH_{rac} and ΔH_R stand for the fusion enthalpy of the racemic and the enantiopure compounds respectively. T denotes the melting point in K. T_{rac} and T_R represent the melting points of the racemic and the enantiopure (*R*) compound respectively, in K units. R is the universal gas constant. Although the calculations

were done using the molar fractions of the enantiopure acid, the obtained models were plotted against the enantiomeric excess, in order to achieve a similar scaling with the $ee_0 - ee_1$ diagrams.

In case of **1** and **2** the phase diagrams calculated based on our measurements are in good agreement with those obtained from the literature. In case of **1**, the measured points were also published in a tabular form, making it possible to present them in the diagram of Fig. 3.[22] Although the reference cited for **2** only contains the measurement points as a diagram, the model fitted excellently to the measured eutectic melting points and melting points.[21] The calculation of the eutectic composition of the enantiomeric mixture of **3** is in good accordance with the measured points, but there is only a fairly good fitting to the measured points of the liquid curve. Furthermore, the eutectic melting point temperature could not be accurately predicted by the model. A possible reason is that the melting point of the racemate and that of the pure enantiomer are very close being a quite unusual behavior of racemic compounds.

It is known that **1** can be produced in a conglomerate form either by using additives or by applying freeze drying as a crystallization method.[25,26] Therefore the crystal structures of the used 2-chloromandelic acid (both the racemate and the pure enantiomer) and the products of the GAS recrystallization were investigated using powder X-ray diffraction. Observing the comparison of the diffractograms in the Supplementary data, we concluded that, among the circumstances of the GAS fractionation process, **1** behaves as a racemic compound.

In order to develop a suitable method to the fast and efficient precipitation of a certain ratio of the dissolved enantiomeric mixture one needs to test the solubility of the studied compounds as a function of pressure, temperature and organic solvent to carbon dioxide ratio. Typical effects of the operational parameters can be found in the literature.[27] Based on the preliminary experiments required, 16 MPa pressure 40 °C temperature, a carbon dioxide to acetonitrile mass ratio of approx. 80 in case of **2** and **3** and 200 in case of **1** were selected. Near saturation solutions of the organic acids in the organic solvent were used in the detailed investigation of the enantiomeric enrichment. After adding the carbon dioxide antisolvent and the extraction phase a solid precipitate was recovered, called raffinate. The average raffinate yield was set by selecting the above conditions in all three cases approximately to 50%. Yields were calculated as recovered mass over the total mass of the starting material.

The results of the gas antisolvent fractionation experiments are shown in the lower sections of Figs 3-5. The dashed lines drawn are only to guide the eye. In all three diagrams non-ideal behavior is observed, showing an intersection of the enantiomeric excess curves of raffinates (precipitated solids), extracts and the $ee=ee_0$ line. We call these intersections limiting composition, being analogous to azeotropic compositions of binary liquid-vapor equilibrium curves. However, it must be noted, that the enantiomeric excesses plotted in these diagrams are not compositions of phases in equilibrium, but initial and product enantiomeric excess values. From a non-racemic mixture of any of the three acids, a crystalline raffinate and an extract (represented in Fig. 3.; Fig. 4; Fig. 5. as a) square and b) dot respectively) can be produced having different enantiomeric purities from each other and from the starting material as well if the initial *ee* is not equal to the limiting composition. This means the occurrence of self-disproportionation of enantiomers under the circumstances of the fluid-solid phase transition occurring during GASF. The limiting compositions show strong correlations to the atmospheric

melting eutectic compositions of the enantiomeric mixtures (compare upper and lower diagrams in Fig 3.; Fig. 4. and Fig. 5.). At enantiomeric purities lower than the limiting *ee*, the extract is optically enriched while the composition of the raffinate gets closer to racemic. At initial *ee*-s exceeding the enantiomeric purity of the eutectic point it is the crystalline raffinate being enriched in the pure (in this case *R*) enantiomer.

The behavior observed at the two sides of the limiting composition is very similar to that observed in case of slow, atmospherical experiments conducted on thermodynamically controlled systems.[5] This behavior suggests that the compositions of the separated products are dominated by an equilibrium. This result is counter-intuitive because under the circumstances of GAS fractionation a high oversaturation occurs in a very short time that could promote the domination of kinetic effects. However, recently analogous observations were found for crystallization habits in supercritical antisolvent systems.[28]

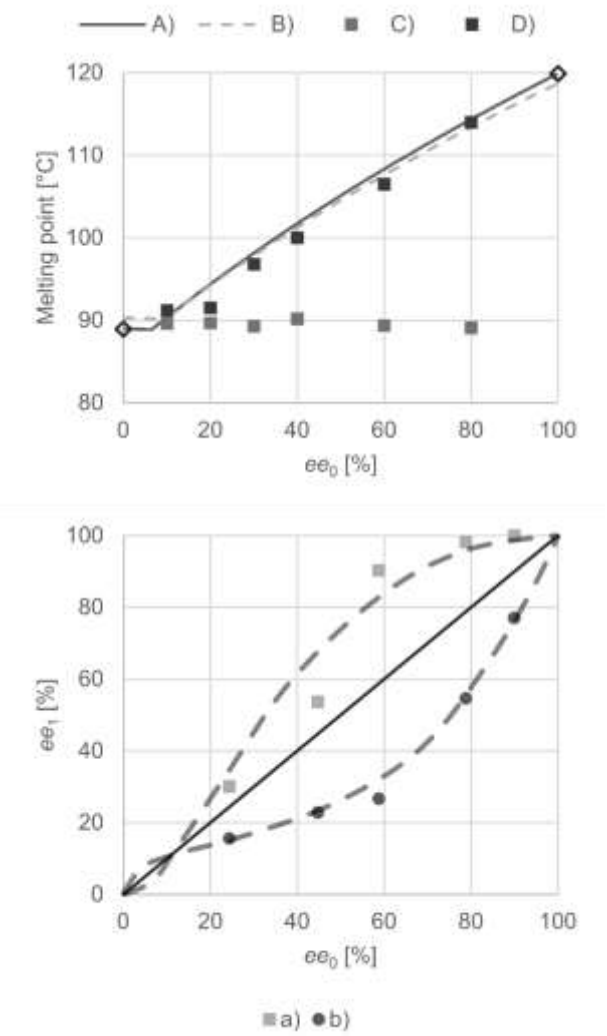

Figure 3. Melting point phase equilibrium diagram (upper) and ee_0 – ee_1 diagram (lower) of **1** (2-chloromandelic acid)

A) Phase equilibrium curve modelled based on measured data

B) Phase equilibrium curve from literature reference [22]

C) Eutectic melting points[22]

D) Melting points[22]

a) Crystalline raffinates

b) Extracts

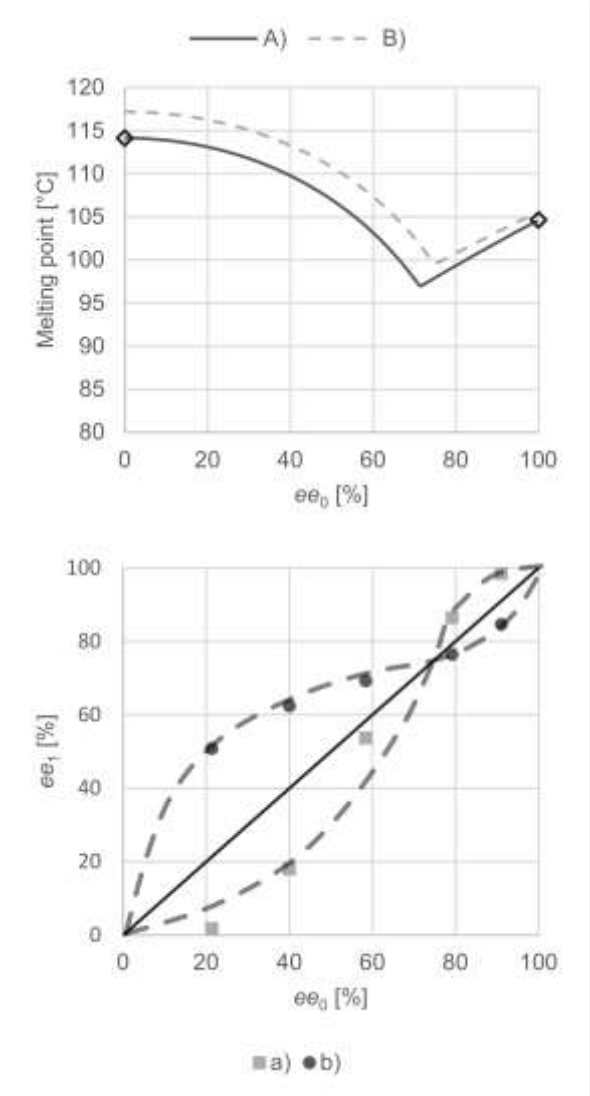

Figure 4. Melting point phase equilibrium diagram (upper) and ee_0 – ee_1 diagram (lower) of **2** (3-chloromandelic acid)

A) Phase equilibrium curve modelled based on measured data

B) Phase equilibrium curve from literature reference [21]

a) Crystalline raffinates

b) Extracts

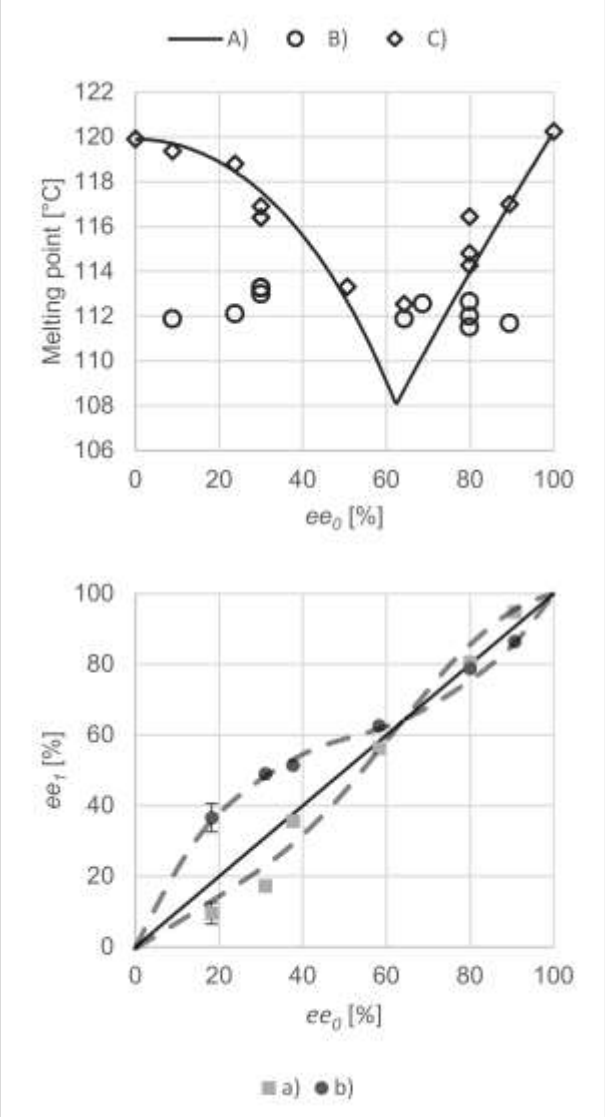

Figure 5. Melting point phase equilibrium diagram (upper) and ee_0 – ee_1 diagram (lower) of **3** (4-chloromandelic acid)
A) Phase equilibrium curve modelled based on measured data
B) Eutectic melting points
C) Melting points
a) Crystalline raffinates
b) Extracts

Atmospheric experiments were also carried out using hexane as an antisolvent, a solvent with the closest polarity and solvent power to those of supercritical carbon dioxide. In case of **1** and **2**, no precipitation was observed after the addition of over 100 mL of hexane to the almost saturated acetonitrile solutions (1 mL in case of **2** and **3**; 0.4 mL in case of **1**) of the racemic

materials. Although **3** (4-chloromandelic acid) precipitated, no enantiomeric enrichment was observed.

3. Conclusion

Gas antisolvent fractionation using supercritical carbon dioxide is an efficient novel method of enantiomeric enrichment. The composition limiting the enantiomeric purification of the non-racemic mixtures of the 2- 3- or 4-chloromandelic acids correlates strongly to the relevant atmospheric melting eutectic enantiomeric composition. Despite the very large oversaturation in a very short time being an inherent condition at GAS fractionation, the composition of the phases obtained during the GAS fractionation is determined by an equilibrium. Atmospheric antisolvent precipitations in contrast only resulted in a crystalline product in one case and failed to enhance the enantiomeric purity of the non-racemic mixture.

4. Experimental

4.1. Materials

Carbon dioxide (purity >99.9%) used in the experiments was purchased from Linde Gas Hungary Co. Cltd. and was used after distillation. Enantiopure (*R*)-2-chloromandelic acid (CAS 52950-18-2), racemic 3-chloromandelic acid (CAS 16273-37-3; purity >97%), racemic 4-chloromandelic acid (CAS 7138-34-3) and (*R*)-4-chloromandelic acid (CAS 32189-36-9) (purities over 98%) were purchased from TCI Co. Ltd. Racemic 2-chloromandelic acid (CAS 10421-85-9; purity >98%) and enantiopure (*R*)-3-chloromandelic acid (CAS 61008-98-8; purity >97%) were purchased from Sigma-Aldrich Co. LLC. Acetonitrile (purity >99%) used as a co-solvent was bought from Reanal Private Ltd. Methanol used in the solvent traps and *n*-hexane used in the atmospheric experiments were purchased from Molar Chemicals Ltd (purities >99%).

4.2. Gas antisolvent fractionation as a method of enantiomeric enrichment

The experimental procedure was very similar in case of all three mandelic acid derivatives. The desired enantiomeric mixtures of the acids were prepared by physically mixing the pure enantiomer and the racemic form. Then the mixture was dissolved in acetonitrile at room temperature to create an almost saturated solution. In case of 2-chloromandelic acid the concentration of the solution was 500 mg/mL, while in the case of 3- and 4-chloromandelic acids it was 200 mg/mL.

A solution containing approx. 100 mg of the acid investigated was filled into a 37 mL laboratory autoclave that was described in a previous communication[29]. The autoclave was tempered at 40 °C and pressurized with a known amount of supercritical carbon dioxide using a Teledyne ISCO 260D syringe pump to 16 MPa. After 1 hour of stirring an extraction step was carried out with carbon dioxide at 16 MPa and 40 °C (100 mL). The total amount of carbon dioxide used in this step was equivalent to 3 times the volume of the laboratory autoclave. Solid particles were held in the reactor using a filter and the dissolved, extracted amount of acid was collected in a methanol trap. The trap is not needed in a scaled-up equipment, as in a larger scale a separator based on pressure reduction is sufficient. After switching off the stirring, the reactor was depressurized. The white crystalline product in the reactor was collected, then its residue was dissolved, collected and dried. The extract was collected by evaporating the solvent from the trap after rinsing the outlet valve and tubing of the reactor with methanol.

4.3. Atmospheric precipitation

As a reference, atmospheric precipitation experiments were also carried out. Almost saturated acetonitrile solutions of approx. 200 mg of the racemic acids were filled in glass flasks and tempered at 40 °C. Then, maintaining constant temperature *n*-hexane was slowly added until precipitation of the acid was visually observable. Only 4-chloromandelic acid showed precipitation. Thus, recrystallization of a 40% *ee* 4-chloromandelic acid (*R*)-enriched enantiomeric mixture was carried out using 100 mL of *n*-hexane. The crystalline product was filtered and washed with 5 mL of *n*-hexane. The solvent from the mother liquor was evaporated.

4.4. Capillary electrophoresis

Samples obtained from the GAS and atmospherical experiments, as well as starting materials were analyzed on an Agilent 7100 capillary electrophoresis equipment fitted with a 50 cm long polyimide-covered uncoated silica capillary. Experiments were performed in a pH 9, 50 mM borate buffer. Peaks were detected using a DAD detector, with a detection wavelength of 200 nm and a reference wavelength of 320 nm. Measurements were carried out at 25 °C with 20 kV voltage applied to the column. To achieve chiral separation, 10 mM of an amino-substituted β-cyclodextrin named 6-Monodeoxy-6-monoamino-beta-cyclodextrin hydrochloride (product of Cyclolab Ltd) was used as chiral selector.

4.5. Melting point measurements

The melting point phase diagrams of the acids were recorded using a TA Instruments 2920 Modulated DSC equipment. Roughly 3 mg sample was filled in an aluminum crucible and sealed. Heating was performed with a rate of 5 °C/min up to 50 °C, then with a rate of 2 °C/min up to 150 °C.

Acknowledgement

We highly appreciate the fruitful discussions with Prof. Elemér Fogassy and the assistance of Klára Sai-Halász in the capillary electrophoretic measurements. Our research work was supported by OTKA [grant number K108979]. E. Sz. thanks to the support provided by the Hungarian Academy of Sciences through the Bolyai Scholarship for Researchers.

1. Soloshonok, V.A.; Klika, K.D. *Helv. Chim. Acta* **2014**; 97 1583-1589.

2. Sorochinsky, A.E.; Soloshonok, V.A. *Topics in Current Chemistry*. Vol 341. Springer: Cham; 2013; pp. 301-339.

3. Soloshonok, V.A.; Ueki, H.; Yasumoto, M.; Mekala, S.; Hirschi, J.S.; Singleton, D.A. *J. Am. Chem. Soc.* **2007**; 129 12112–12113.

4. Soloshonok, V.A.; Roussel, C.; Kitagawa, O.; Sorochinsky, A.E. *Chem. Soc. Rev.* **2012**; 41 4180-4188.

5. Faigl, F.; Fogassy, E.; Nógrádi, M.; Pálovics, E.; Schindler, J. *Org. Biomol. Chem.* **2010**; 8 947-959.

6. Esfandiari, N. *J. Supercrit. Fluids* **2015**; 100 129-141.

7. Knez, Ž.; Knez Hrnčič, M.; Škerget, M. *Annu. Rev. Chem. Biomol. Eng.* **2015**; 6 379-407.

8. Pasquali, I.; Bettini, R. *Int. J. Pharm.* **2008**; 364 176-187.

9. Martín, V.; Romero-Díez, R.; Rodríguez-Rojo, S.; Cocero, M.J. *Chem. Eng. J.* **2015**; 279 425-432.

10. Teberikler, L.; Koseoglu, S.; Akgerman, A. *J. Food Sci.* **2001**; 66 850-853.

11. Marqués, J.L.; Della Porta, G.; Reverchon, E.; Renuncio, J.A.R.; Mainar, A.M. *J. Supercrit. Fluids* **2013**; 82 238-243.

12. Floris, T.; Filippino, G.; Scrugli, S.; Pinna, M.B.; Argiolas, F.; Argiolas, A.; Murru, M.; Reverchon, E. *J. Supercrit. Fluids* **2010**; 54 165-170.

13. Sánchez-Camargo, A.P.P.; Mendiola, J.A.A.; Valdés, A.; Castro-Puyana, M.; García-Cañas, V.; Cifuentes, A.; Herrero, M.; Ibáñez, E. *J. Supercrit. Fluids* **2016**; 107 581-589.

14. Bánsághi, G.; Lőrincz, L.; Szilágyi, I.M.; Madarász, J.; Székely, E. *Chem. Eng. Technol.* **2014**; 37 1417-1421.

15. Martín, A.; Cocero, M.J.J. *J. Supercrit. Fluids* **2007**; 40 67-73.

16. Wu, J.; Liu, F.; Wang, S.; Wang, H.; Liu, Q.; Song, X.; Li, J.; Xu, L.; Tan, W. *Chirality* **2016**; 28 306-312.

17. Davis, G.C.; Kong, Y.; Paige, M.; Li, Z.; Merrick, E.C.; Hansen, T.; Suy, S.; Wang, K.; Dakshanamurthy, S.; Cordova, A.; McManus, O.B.; Williams, B.S.; Chruszcz, M.; Minor, W.; Patel, M.K.; Brown, M.L. *Bioorg. Med. Chem.* **2012**; 20 2180-2188.

18. Zavakhina, M.S.; Samsonenko, D.G.; Dybtsev, D.N.; Fedin, V.P. *J. Struct. Chem.* **2014**; 55 1442-1447.

19. Tashiro, Y.; Nagashima, T.; Aoki, S.; Aboshi, Y. Patent number: EP 0009722 B1 **1983**

20. Liu, X.; Yi, Z.; Wang, J.; Liu, G. *RSC Adv.* **2015**; 5 10641-10646.

21. Zhang, Y.; Ray, A.; Rohani, S. *Chem. Eng. Sci.* **2009**; 64 192-197.

22. He, Q.; Zhu, J.; Gomaa, H.; Jennings, M.; Rohani, S. *J. Pharm. Sci.* **2009**; 98 1835-1844.

23. Collet, A.; Jacques, J. *Bull. Soc. Chim. Fr.* **1973**; 12 3330-3334.

24. von Langermann, J.; Temmel, E.; Seidel-Morgenstern, A.; Lorenz, H. *J. Chem. Eng. Data* **2015**; 60 721-728.

25. Davey, R.J.; Sadiq, G.; Back, K.; Wilkinson, L.; Seaton, C.C. *Chem. Commun. (Camb).* **2012**; 48 1976-1978.

26. He, Q.; Rohani, S.; Zhu, J.; Gomaa, H. *Cryst. Growth Des.* **2010**; 10 5136-5145.

27. Foster, N.R.; Gurdial, G.S.; Yun, J.S.L.; Liong, K.K.; Tilly, K.D.; Ting, S.S.T.; Singh, H.; Lee, J.H. *Ind. Eng. Chem. Res* **1991**; 30 1955-1964.

28. Kőrösi, M.; Székely, E.; Madarász, J.; Sohajda, T. In *16th European Meeting on Supercritical Fluids*. Lisbon; 2017.

29. Kőrösi, M.; Madarász, J.; Sohajda, T.; Székely, E. *Chirality* 2017 1-6.